JOURNAL OF Applied Polymer SCIENCE

Properties of Recycled Polycaprolactone-Based Thermoplastic Polyurethane Filled with Montmorillonites

Kristina Žukienė,[1] Virginija Jankauskaitė,[1] Vitalija Betingytė,[1] Arūnas Baltušnikas[2]

[1]Department of Clothing and Polymer Products Technology, Kaunas University of Technology, Studentų 56, LT-51424 Kaunas, Lithuania

[2]Department of Silicate Technology, Kaunas University of Technology, Radvilėnų 1, LT-50254 Kaunas, Lithuania

Correspondence to: V. Betingytė (E-mail: vitalija.betingyte@stud.ktu.lt)

ABSTRACT: The properties of recycled low temperature biodegradable polycaprolactone-based thermoplastic polyurethane (rTPU), filled with different types of organically modified montmorillonite (MMT) prepared by two-roll milling, were studied. The dependence of rTPU properties on the mastication time and clays content was determined by various structural and physical testing methods. Results show that the melt flow and mechanical properties of rTPU deteriorate with increasing of mastication time, but thermal properties were affected only slightly. rTPU/MMT composites show exfoliated or intercalated structures depending on the nature of organic modifier of clay. MMT reduces slightly rTPU tensile and melt flow properties, but accelerates hydrolytic degradation process. During degradation the weight loss and polydispersity increase significantly in the presence of MMT, but it does not accelerate crystallinity changes. The degradation of rTPU composites with higher hydrophilicity organoclays proceeds faster than that with hydrophobic ones due to the relatively higher interaction with polymer matrix. © 2012 Wiley Periodicals, Inc. J. Appl. Polym. Sci. 000: 000–000, 2012

KEYWORDS: clay; degradation; recycling; biodegradable; nanocomposites

Received 23 March 2012; accepted 27 July 2012; published online
DOI: 10.1002/app.38408

INTRODUCTION

The degradation of most plastic products after the end of their exploitation time is limited. Most of them are highly resistant to microbial degradation or deterioration and, therefore, become new environmental polluters. Polymer recycling is an environmentally attractive solution, but it will not yield enough quality of products due to the heterogeneous nature of plastics. Furthermore, some plastics are not economically feasible to recycle. These facts lead to synthesis and manufacture of biodegradable polymers.

Biodegradable polyurethanes are an important class of biomaterials due to their excellent physical properties and relatively good biocompatibility. Their mechanical properties and biodegradability can be tailored for different applications by varying the chemistry and molecular weight of their components.[1] Generally polyurethane is prepared from the isocyanate and polyol, such as polyester and/or polyether. They form multiblock copolymers consisting of alternating urethane based hard segment and polyether and/or polyester soft segment. The hard segment provides dimensional stability by acting as reinforcing filler and as thermally reversible crosslinker. The soft segment provides the elastomeric character to the polymer backbone.[2]

In the case of polycaprolactone (PCL) based thermoplastic polyurethanes (TPU), PCL usually forms soft segments.[2,3] PCL is semicrystalline linear aliphatic polyester derived from a ring opening polymerization of ε-caprolactone having relatively low melting point, about 60–65°C.[4] In the family of polyesters PCL is considered as biodegradable polymer with adequate mechanical properties.[5,6] However, PCL has long-term degradation—up to 3–4 years due to the hydrophobicity and crystallinity.[7] The hydrolytic degradation of PCL takes place through the hydrolysis of the ester backbone, as in the case of other aliphatic polyesters, in a random fashion under aqueous conditions and depends on the crystallinity, size and shape of crystallite, the morphological structure, etc.[1,3] The degradation occurs preferentially in the amorphous region rather than in the crystalline one. Similarly, hydrolytic degradation of thermoplastic polyurethane takes place through the hydrolysis of the ester backbone of the PCL soft segment.[8]

The biodegradability of polymers can be easy improved by adding nanofillers, such as nanoclays.[9–12] The nanoclay belongs to the family of layered silicates (montmorillonite, saponine, hectorite) and is the most commonly used nanofiller for the design of polymeric nanocomposites with greatly improved physical,

Table I. Main Properties of used Polycaprolactone-based Thermoplastic Polyurethane

			Tensile properties		
Commercial name	Code	T_g (°C)	Yield point σ_Y (MPa)	Tensile strength σ (MPa)	Elongation at break ε (%)
Beachcast	TPU-1	60–65	17.6	24.1	2700
Turbotreat	TPU-2	70–75	16.0	29.6	685
Beachcast: Turbotreat	TPU-1 : TPU-2 = 60 : 40 wt %	64–68	16.9	25.4	2245

mechanical, and biodegradability properties.[13–15] It must be pointed out that for polymer/layered silicate systems the enhancement of the afore-mentioned properties strongly depends on the obtainment of effective nanometer-scaled dispersion of the filler into the polymer matrix.[10]

Among the family of layered silicates, montmorillonite (MMT) is most commonly used in polymer/nanoclay materials.[16–18] MMT consist of two silicates tetrahedrons fused to an edge-shared octahedral sheet of either aluminum or magnesium hydroxide. The thickness of the layer is around 1 nm and its lateral dimensions may vary from 30 nm to several microns or even more.[10]

The small amount of nanosized MMT platelets (up to 5 wt %) can increase the mechanical and physical properties of polymers, including strength and stiffness, heat and UV resistance, while maintaining transparency and impact property.[1,13,16] MMT is usually chemically modified due to its hydrophilicity and incompatibility with most organic materials.[14] Generally, this can be done by ion-exchange reactions with cationic surfactants, including primary, secondary, tertiary, and quaternary alkylammonium cations.[19] This modification also leads to the expanding of the spacing between the silicate layers due to intercalated of alkyl chain in the interlayer.

Morphology as well as mechanical properties of polymer nanocomposites depends largely on the method of production.[13] Usually used methods of preparation of nanocomposites from elastomers and thermoplastic are *in situ* polymerization, melt intercalation, and solution mixing technique.[16,20–22] However, there are not many studies on the incorporation of the nanofillers by two-roll milling process. The two-roll mill mixing technique has become the promising method for fabricating polymer/clay nanocomposites because of the many advantages including the use of existing processing equipment and its eco-friendly acceptable nature.[23] Meanwhile, manufacturing of layered silicate nanocomposite with two-roll mill is used only seldom.

Low-temperature TPU is used for short-life orthopedic devices due to the shape memory properties, high flexibility, and biocompatibility.[24] However, the biomedical application of TPU creates large amount of production waste. The possibility of recycling and secondary use of TPU was investigated in Ref. 25. It has been found that recycled TPU blends have good mechanical properties compared with the pristine materials and can be repeatedly used for orthopedic splint production.

The aim of this study is to determine the effect of organically modified MMTs on the recycled polycaprolactone-based thermoplastic polyurethane morphology changes, mechanical properties and hydrolytic degradation.

EXPERIMENTAL

Materials

The waste from low temperature polycaprolactone-based thermoplastic polyurethane (TPU) *Beachcast* and *Turbotreat* (T-Tape Company, Netherlands) was used for investigations. The material was obtained from orthopedic device manufacturing process. The waste was generated at the cutting step. The main properties of these commercially available TPU are presented in Table I. Both TPU have similar glass transition temperatures. Higher tensile strength is characteristic for *Turbotreat*, while *Beachcast* shows significantly higher elongation at break.

The blends obtained by the mixing of various TPU types show intermediate flexural and tensile properties compared to that of the pristine blend components.[25] Therefore, the recycled blend of *Beachcast/Turbotreat* = 60/40 wt % (rTPU) was used for further investigation. The main properties of that rTPU are presented in Table I.

For preparation of the nanocomposites organoclays were selected. Three types of organically modified MMT clays Cloisite 10A (C10A), Cloisite 15A (C15A), and Cloisite 30B (C30B) were kindly provided by Souther Clay Products (Gonzales, TX). All types of organoclays were surface-treated by ion exchange reaction between Na^+ existing in the gallery of the nanoclay and quaternary ammonium cations. C10A was modified with dimethyl benzyl(hydrogenated tallow alkyl) ammonium cations, C15A—with dimethyl di(hydrogenated tallow alkyl) ammonium cations, while C30B was treated with bis-(2-hydroxyethyl) methyl (hydrogenated tallow alkyl) ammonium cations. The main characteristics of these MMT clays, obtained from data sheets, are listed in Table II. C30B has the lower cation exchange capacity (CEC) compared to all investigated clays; therefore, separation of platelet is easier than in the case of other clays. The organoclays ranked in terms of increasing hydrophilicity as follows: C30B > C10A > C15A.

Preparation of Samples

The rTPU waste blends were obtained by 600 s mastication on the open mill PD 320 with friction of 1.25. After that the organoclay was added and milling was continued over 600 s. The temperature of the mill was 55°C; it was controlled by means of cold water running inside the rolls.

The rTPU/organoclay composites were prepared by changing filler content from 1 wt % up to 5 wt %.

Table II. Characteristics of Commercial Organoclays[a]

Characteristic	Cloisite 10A	Cloisite 15A	Cloisite 30B
Code	C10A	C15A	C30B
Basal spacing d_{001}, nm	1.92	3.15	1.85
Organic modifier[b]	2MBHT	2M2HT	MT2EtOH
Structural formula	$(CH_3)_2(HT)(CH_2C_6H_5)N^+$	$(CH_3)_2(HT)_2N^+$	$(CH_3)(T)(CH_2CH_2OH)_2N^+$
Organic modifier concentration, meq/100 g	125	125	90
Counterion	Chloride	Chloride	Chloride
Hydrophobicity	Low	High	Very low

[a]According to the manufacturer, [b]Quaternary ammonium chlorides: 2MBHT—alkyl(benzyl)dimethyl, 2M2HT—dialkyldimethyl, MT2EtOH—alkylbis (2-hydroxyethyl)methyl. T = tallow (65% C18, 30% C16, 5% C14), HT = hydrogenated tallow.

The test samples of composites were prepared by the compression molding. The polymer was placed in the mold with the cavity dimensions of 150 × 130 × 2 mm^3, softened at the temperature of $T = 70$°C for 5 min and then pressed at 4.9 MPa for 2 min. The molds after removing pressure were cooled at room temperature. The specimens were die-cut from the compressed sheet and used for testing after 3 days of storage at room temperature.

Differential Scanning Calorimetry

Differential scanning calorimetry (DSC) (DSC Q10 V9, 0 Build 275 (TA Instruments, USA)) was used to determine the melting/crystallization behavior of the TPU. Temperature heating/cooling cycles from −100°C to +250°C were performed at 10 and 5°C min^{-1}, respectively.

X-Ray Diffraction Analysis

Wide angle X-ray diffraction (XRD) analysis of materials was performed using a diffractometer DRON-6 equipped with a copper target ($\lambda = 1.54$ Å) and flat diffracted beam pyrolitic graphite monochromator. Diffraction patterns were recorded at 35 kV and 20 mA. Scanning was carried out in the 2θ range 2°–70° at the step size of 0.02° (2θ) and counting time of 0.5 s step^{-1}. The diffraction patterns were obtained automatically by data acquisition system.

XRD technique was used to determine the spaces between structural layers of the silicate utilizing Bragg's law:

$$\sin\theta = n\lambda/2d, \tag{1}$$

where λ corresponds to the wavelength of the X-ray radiation used in the diffraction experiment, d is the spacing between diffraction lattice planes, and θ is the measured diffraction angle.

The XFIT program was used for XRD quantitative analysis.[26] The crystallinity of samples was determined by the following equation:

$$W_c = \frac{A_c}{A_c + A_a}, \tag{2}$$

where A_c is the crystalline peak area and A_a is the amorphous halo area.

Scanning Electron Microscopy

SEM analysis was performed using the microscope Quanta 200 FEG (FEI, Netherlands) at 10 or 20 keV. It has 1.5-nm resolutions, high output thermal field emission (>100 nA beam current) with high sensitivity (18 mm) backscatter detector for atomic number contrast.

Mechanical Properties

Dumbbell-shaped specimens for tensile tests were prepared from compressed sheet using appropriate punch. Tensile tests were carried out at room temperature using universal testing machine H25KT with load cell of 1 kN (Tinius Olsen, England). A cross-head speed of 100 mm min^{-1} was used. Measurements were performed at the room temperature with the specimens having gage area of 10 mm × 10 mm and thickness of 2 ± 0.1 mm. Six specimens were tested for each set of samples.

Hydrolytic Degradation

The samples with dimensions of 10 × 10 × 2 mm^3 were placed in 3% NaOH solution. After a predetermined time of ageing the hydrolytically degraded samples were removed, washed with distilled water, and completely dried at 25°C. The degree of degradation was determined from the weight loss according to:

$$\Delta W = \frac{W_0 - W_t}{W_0} \cdot 100, \tag{3}$$

where W_0 is the dry weight of sample before testing, W_t is the dry weight of samples after time t of degradation.

Melt Flow Index

Melt flow index (MFI) is defined as the weight of polymer, in grams, flowing in 10 min through a capillary of a specific diameter and length by a pressure applied via prescribed alternative gravimetric weights for alternative prescribed temperatures. MFI was determined by plastometer (Bita STR-1) with capillary die diameter of 2.095 ± 0.005 mm, when a fixed pressure is applied to the melt via a piston and a load of total mass of 2.16 kg (P = 21.168 N). Tests were carried out at temperature 180°C. MFI was calculated according to the equation:

$$\mathrm{MFI} = 600 \cdot \frac{m}{t}, \tag{4}$$

where m is weight, t is test time.

Molecular Weight

Average molecular weight and dispersity of rTPU and its composites were estimated by the use of size exclusion

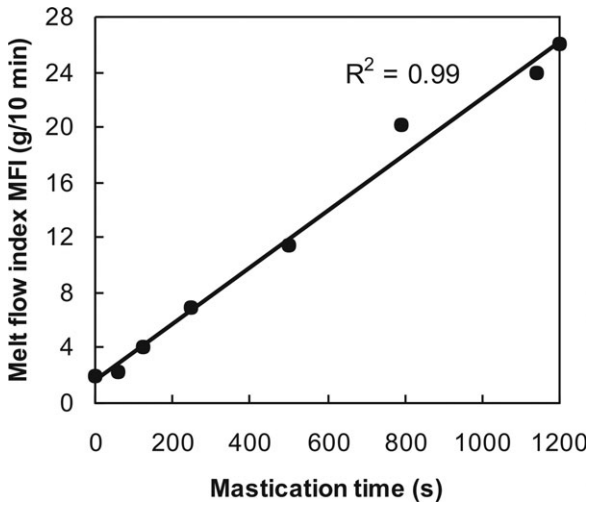

Figure 1. Dependence of TPU melt flow index upon mastication time (test temperature $T = 180°C$, load $P = 21.168$ N).

chromatography (SEC) technique on a instrument Viscotek (GPC Pump VE1122, Dual channel in Line Solvent degasser VE7510-02, Viscotek 270-03 RALS/LALS, VE-3580 RI, and Knauer Smartline Photo diode UV Detectors) equipped with SEC Viscotek T5000 column (exclusion limit 4 000000 MW). Tetrahydrofuran was used as a solvent with flow rate of 1 cm^3 min^{-1} at 60°C. Polystyrene standard of low dispersity (Malvern Poly-CAL PS Std—PS99K) was used to calibrate Viscotek 270-03 RALS/LALS detector.

RESULTS AND DISCUSSIONS

Recycling of rTPU

During recycling process a material undergoes various operations that bring out several modifications in the molecular structure. As a matter of fact, the mechanical properties of the recycled products and their structural organization can be quite different compared to those of pristine materials.

In Figure 1 melt flow index of TPU is reported as a function of the mill mastication time, at 180°C temperature and load of $P = 21.16$ N. As the mastication time increases, MFI increases. It can be related to the TPU chain scission, which is known as chemical reaction resulting in the breaking of skeletal bonds of polymer. It is evident that MFI changes proceed according to the linear law.

DSC was used to determine thermal properties of pristine and recycled TPU. In the tested temperature range (–100°C to +250°C) for thermograms two primary regions—crystallization and melting—are characteristic (Figure 2). In the crystallization region the rTPU chains begin to misalign and lose heat stored in their bonds, while in the melting region it absorbs high amount of energy causing materials flow. It was found that thermal properties of the rTPU are worsened only slightly, but remained comparable with those of pristine TPU. rTPU displays the crystallization exothermic peak at the temperature of about 35°C, while TPU—at 31°C. The endothermic peaks of TPU and rTPU melting lie in the temperature of 68 and 60°C, respectively.[27]

The changes of mechanical properties of TPU during mill mastication were assessed through flexural and tensile properties (Figure 3). The recycling worsens slightly TPU mechanical properties. The increase of mill mastication time up to 1200 s decreases flexural and tensile modules in 25 and 35%, respectively [Figure 3(a)] and flexural and tensile strength decreases in 44 and 32%, respectively [Figure 3(b)]. The higher degree of decrease is observed in the case of the flexural and tensile strength of the rTPU. It must be mentioned, that higher mechanical properties decrease is obtained in the beginning of the mastication time (up to 100 s).The elongation at break decreases, also (about 20% compared to that of pristine TPU).[27]

Dispersion of the Organoclays in rTPU Matrix

The structure of composites of MMT was determined by XRD technique analyzing the diffraction intensity at the diffraction angle based on the interlayer spacing. The XRD results at lower angle ($2 < 2\theta < 10°$) of rTPU, MMT clays and rTPU/MMT composites containing 5 wt % of organoclay are shown in Figure 4. The interplanar spacings of C10A, C15A, and C30B organoclay layers determined by XRD are $d_{001} = 1.96$ nm ($2\theta = 4.50°$), $d_{001} = 3.39$ nm ($2\theta = 2.60°$), and $d_{001} = 1.87$ nm ($2\theta = 4.72°$), respectively, which agree with data presented in materials data sheets. It can be stated that organic modification causes interlayer expansion in C10A and C30B organoclays, but C15A has more disordered structure. No peak within 2θ range of 2°–10° was observed in rTPU samples.

The structure of the rTPU/MMT composites were determined by analyzing the position, shape and the intensity of basal reflections from silicate layers (Figure 4). Generally, the interlayer spacing of the organoclay in polymer depends on the composites preparation method, nature of organoclay and the interaction between the polymer matrix and the organoclay.[16,28] The XRD pattern of rTPU/C10A nanocomposites shows that the d_{001} peak at $2\theta = 4.50°$ of C10A shifted toward lower angles

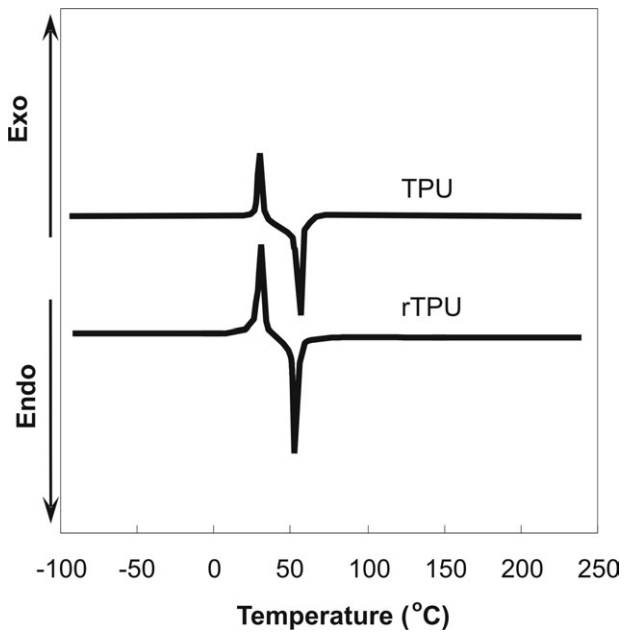

Figure 2. DSC thermograms for pristine and recycled TPU.

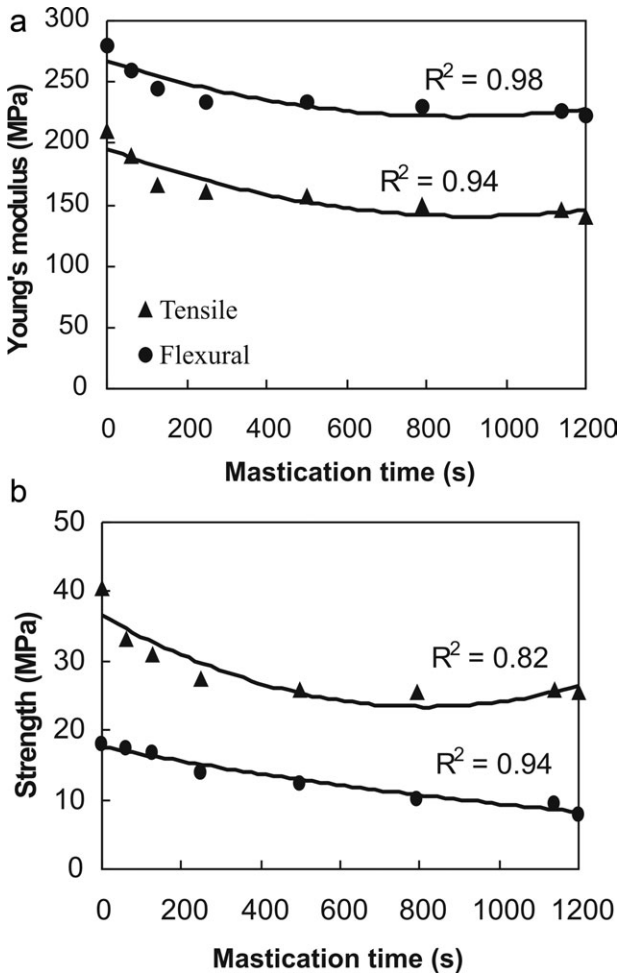

Figure 3. Dependence of recycled TPU flexural and tensile properties on mastication time: (a) Young's moduli; (b) strength.

3.94° although the intensity is strongly reduced indicating the formation of intercalated nanocomposite. Besides, new peak at low angle 2.16° (d_{001} = 4.08 nm) appeared, which means silicate have at least two kinds of dispersion states in the polymer matrix. In the case of rTPU/C15A composite the diffraction peak is only slightly shifted toward lower angle 2.28°, indicating that the silicate structure is affected only negligibly. It also gives a broader peak at higher angles 2θ = 4.50°.

In the case of rTPU/C30B nanocomposite the main diffraction peak of C30B is not detectable in the XRD diffractograms. It is associated with formation of exfoliated structures, when nanoclay layers are well separated from one another by rTPU chains. C30B nanoclay layers separation disrupts coherent layer stacking and results in the featureless diffraction pattern, because the ordering does not present.

The differences between C10A, C15A and C30B clays can be explained by influence of ammonium cations located in the gallery of silicate layers. C15A nanoclay shows highest initial gallery spacing (about 3.39 nm), allowing easier intercalation of the rTPU chains. However, the ammonium cations with two tallow groups are too hydrophobic and, therefore, C15A does not match with the polarity of rTPU. As the result, the lack of strong polar interaction between the ammonium cations in C15A and rTPU chains prevents polymer intercalation.

In the case of the C30B due to the existing of two hydroxyethyl groups, the ammonium cations are the most hydrophilic and have strong polar interaction with the polar groups (i.e., urethane groups) presented in polymer matrix, facilitating the delamination of clay layers and the formation of rTPU/C30B nanocomposites.

It is expected that moderate polarity of C10A is responsible for the formation of intercalated rTPU nanocomposites. The replacement of one hydrogenated tallow group by benzyl group gives C10A the lower hydrophobicity and higher compatibility comparing to that of C15A.

Properties of rTPU/MMT Composites

It was found that melt flow index of composites decreases, but decrease level depends on the type of MMT (Figure 5). MMT increases the rTPU viscosity and reduces the MFI. The 5 wt % of organoclay decrease MFI values of rTPU composites about 20–38% compared with unfilled rTPU. The decrease of MFI may occur due to the increase of friction between the rTPU melt and the MMT particles. In addition, the decrease of MFI in rTPU/C30B can be related to higher intermolecular interaction between the polymer chains.

Table III shows the comparison of the mechanical properties of various rTPU/MMT composites. Modulus at break *E* of all

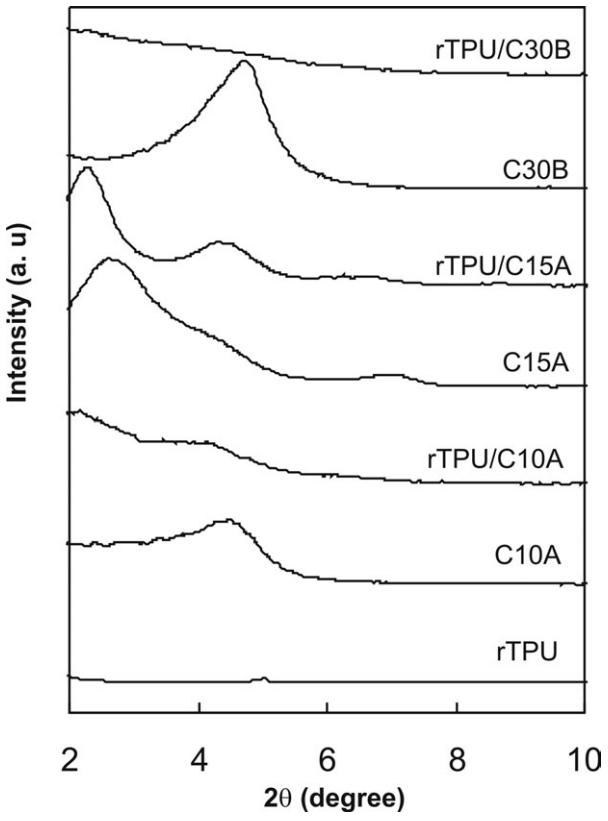

Figure 4. X-ray diffractograms for rTPU, different MMT clays, and rTPU/MMT composites with 5 wt % of clay.

Applied Polymer SCIENCE

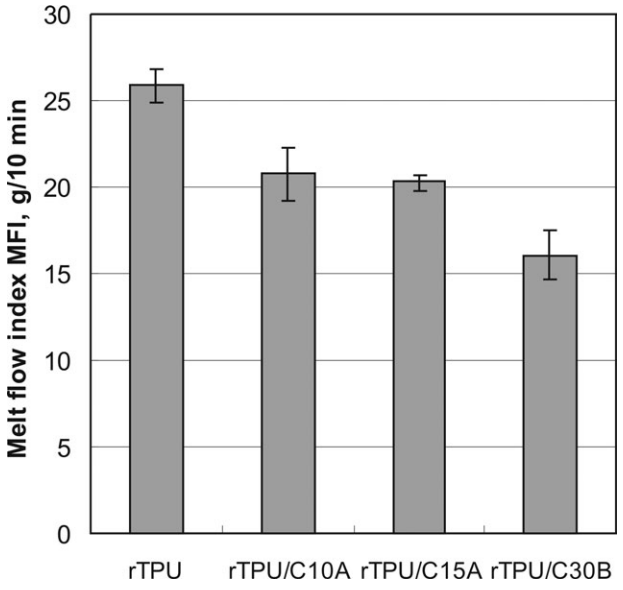

Figure 5. Melt flow index of TPU and rTPU composites (rTPU/MMT = 95/5 wt %) when test load $P = 21.168$ N, temperature $T = 180°C$.

tested rTPU/MMT composites increases with the increase of MMT content. In the case of 5 wt % of organoclays rTPU/C10A, rTPU/C15A, and rTPU/C30B composites modulus increases in 34, 36, and 20%, respectively. This was accompanied by the slightly decrease in tensile strength (10–14%) and elongation at break (7–10%). The rTPU/C10A and rTPU/C30B nanocomposites in comparison with rTPU/C15A possess lower degree of decrease. It may be attributed to the intercalation for C10A and exfoliation of C30B in the rTPU matrix.

Hydrolytic Degradation of rTPU/MMT Composites

Weight Loss. To understand the effect of organoclay on the degradability of rTPU matrix, hydrolytic degradation test in 3% NaOH solution at different immersion time was performed. The results are shown in Figure 6, where the weight loss of rTPU and rTPU composites is plotted against the time of degradation. It was found that the weight loss increases with the increase of degradation time. The rTPU is resistant to the hydrolytic degradation till 400 h of immersion, possessing weight loss barely in 1.6%.

The degradation of the rTPU/MMT composites proceeds in higher rate and depends on the hydrophobicity and content of used organoclays. Generally, the increase of degradation rate can be attributed to the presence of hydroxyl groups on the edges of MMT, which can catalyze the hydrolysis reactions of the polymeric matrix.[16] The degradation of the rTPU/C30B nanocomposite proceeds significantly faster. Such behavior can be explained by the relatively higher hydrophilicity of C30B compared with C10A and C15B. Hydrophobic filler C15A in content of 5 wt %, decreases weight of rTPU matrix in 1.3 times after 670 h of degradation in NaOH solution [Figure 6(b)], while rTPU with C10A and C30B degrades 3.4 and 13 times faster, respectively [Figure 6(a, c)]. The hydrophilicity of these clays allows the water molecules to penetrate more easily within the materials and to cause their hydrolytic degradation. The increase of C30B content up to 10 wt % still further intensifies the degradation process of nanocomposite. It may be supposed that the higher volume of the polymer matrix in contact with the nanoclay surface would result in easier water attack of the polymer chains comparing to the unfilled polymer.

As it can be seen from the above presented data, the C30B clay has more significant influence on the hydrolytic degradation and mechanical properties of rTPU than other clays (C15A, C10A), consequently only that kind of clay was used for further morphological and molecular weight investigations of the rTPU nanocomposites.

Morphology. The rTPU nanocomposites surface morphological evolution during the hydrolysis process performed by SEM is presented in Figure 7. It was obtained that due to the high level of rTPU/C30B = 95/5 wt % samples degradation, rTPU surface view is not informative. Therefore, the SEM images of rTPU/C30B = 95/3 wt % nanocomposite are presented. Even low magnification (600×) confirms the considerable level of surface degradation. Before degradation the rTPU/C30B surface has some roughness due to the samples formation procedure [Figure 7(a)]. As degradation proceeds, the surface become more rugged, because the top layer of samples is gradually removed.

Table III. Tensile Properties of Various rTPU/MMT Composites

Nanocomposite	Organoclay content (wt %)	Modulus at break E (MPa)	Tensile strength σ (MPa)	Elongation at break ε (%)
rTPU/C10A	0	29.51 ± 1.35	25.41 ± 0.80	2245 ± 63
	2	30.92 ± 1.35	24.14 ± 0.94	2134 ± 10
	3	32.63 ± 0.79	23.68 ± 0.74	2108 ± 57
	5	38.80 ± 1.14	22.95 ± 0.65	2092 ± 67
rTPU/C15A	2	32.24 ± 1.54	24.48 ± 0.39	2168 ± 77
	3	34.78 ± 1.12	22.62 ± 0.79	2073 ± 76
	5	39.37 ± 0.86	22.06 ± 0.70	2021 ± 81
rTPU/C30B	2	33.70 ± 1.17	23.98 ± 0.99	2172 ± 57
	3	34.32 ± 0.57	23.47 ± 0.32	2147 ± 49
	5	35.07 ± 1.72	22.90 ± 0.26	2105 ± 11

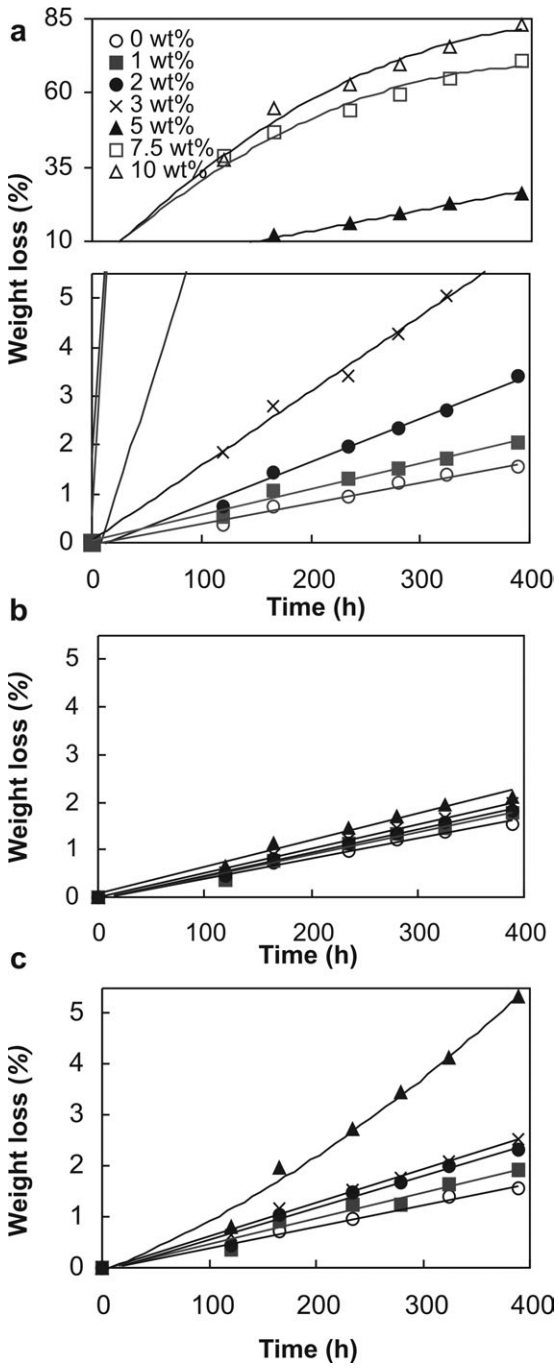

Figure 6. Dependence of rTPU weight loss on the type and content of organically modified MMT: (a) C30B; (b) C15A; (c) C10A.

As a result of surface erosion, the micrometer-sized particles aggregates could be seen in the samples after 400 h degradation [Figure 7(b)]. It was noted[29] that polymer/clay composites degradation starts at the interface between polymer matrix and fillers. Therefore, believable that markedly higher surface magnification (5000×) can reveal the changes in morphology of degraded composites (Figure 8). Even after 50 h of hydrolytic degradation of rTPU/C30B = 95/3 wt % nanocomposites some pits and single cracks were observed (it is not showed). The cracks number increases with the increase of samples immersion time in NaOH solution. At degradation time of 150 h the hydrolytic attack on the sample seems to be occurring layer by layer and zigzag-pattern pits with area of about 6–12 μm^2 in the polymer matrix are observed [Figure 8(b)]. The missing material can be corresponded to the diffusion of low molecular weight constituents into the surrounding environment as the rTPU hydrolyzed. The degradation of 400 h reveals clearly evident small residual aggregates (ca. 2 – 7 μm) of nanoclay [Figure 8(c)]. It confirms not enough dispersion level of organoclay C30B. It can be stated that the C30B layers were not all well exfoliated and distributed in the rTPU matrix. The increasing mixing time would results in improved exfoliation of clay particles.

The maintenance of long time degradation (800 h) causes the decrease in sample thickness as well as significant surface morphological roughness due to the further pits formation with cavities dimension of 20 μm [Figure 8(d)].

Molecular Weight. Degradation behavior of rTPU and its nanocomposites with 5 wt % of C30B was investigated through molecular weight measurements. Table IV and Figure 9 shows changes of weight-average molecular weight (M_w), number-average molecular weight (M_n), and polydispersity (M_w/M_n) of rTPU and rTPU/C30B nanocomposites after 670 h of the degradation. The analysis clearly shows that the obtained curves are not monomodals with comparatively broad molecular weight distribution. As can be seen, the hydrolytic degradation of rTPU caused a some increase in M_w and decrease in M_n that could be attributed to the chain crosslinking and scission [Figure 9(a)], while rTPU/C30B molecular weight decreases during degradation [Figure 9(b)]. SEC analyses suggest that MMT intensifies the hydrolytic degradation rate of rTPU by enhancing the breakdown of the high molecular weight species in to low molecular weight molecules increasing polydispersity. The polydispersity M_w/M_n of rTPU increases by six times after 670 h of hydrolytic degradation, whereas that of rTPU/C30B nanocomposite increases by seven times. All the above results suggest that nanoclay intensifies the reduction of the molecular weight of the rTPU polymer during hydrolytic degradation.

Crystallinity. As in the case of aliphatic polyesters,[1,3,5] the degradation of the rTPU take place through the hydrolysis of the ester backbone of the polycaprolactone in the soft segment. Because the rTPU/C30B = 95/5 wt % nanocomposites have experienced weight loss from hydrolysis, the increase in crystallinity can be expected.

The changes in the crystallinity were evaluated by X-ray analysis. Figure 10 shows the XRD patterns (2θ value 10° to 40°) of rTPU and rTPU/C30B nanocomposites before and after 400 and 670 h of hydrolytic degradation. The crystalline structure of rTPU is retained in presence of clays, but peak intensities at 2θ = 21.4 and 23.7° have been reduced in rTPU/C30B nanocomposite exhibiting less crystallinity than matrix. It is known that MMT reduces the amount of crystalline structures, and, thereby, increases the amount of amorphous zones between the crystalline structures of TPU.[15,30,31]

From Figure 11 can be seen that the crystallinity of rTPU matrix and rTPU/C30B = 95/5 wt % nanocomposite during the

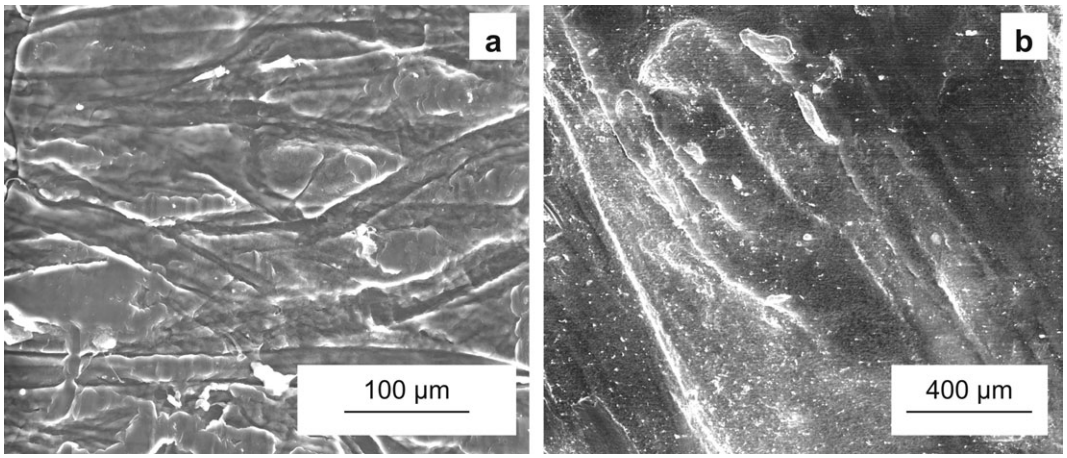

Figure 7. SEM images of rTPU surface with 3 wt % of C30B before (a) and after hydrolytic degradation at 400 h (b) (magnification of ×600).

hydrolytic degradation time tested increases around twice—in the case of rTPU crystallinity changes from 6.1 up to 12.6% (2.1 times), while in the case of rTPU/C30B with 5 wt % of clay—from 4.1% up to 7.1% (1.7 times). Thus, the C30B clay even retards the rate of crystallinity change during degradation.

The increase in crystallinity after degradation of semicrystalline polymers including PCL based polyurethanes has been reported in few studies.[2,3,9,32] Rodrigues da Silva et al.[2] noted that the increase of crystallinity of PCL-based biodegradable polyurethanes is a result of the hydrolysis of PCL ester bonds that enhances the mobility and freedom of lower molar mass chains and, consequently, their ability to pack in a crystalline structure. On the other hand, according to Rutkowska et al.,[32] the increase of crystallinity of PCL after biodegradation can be explained by removing of the part of the amorphous phase by

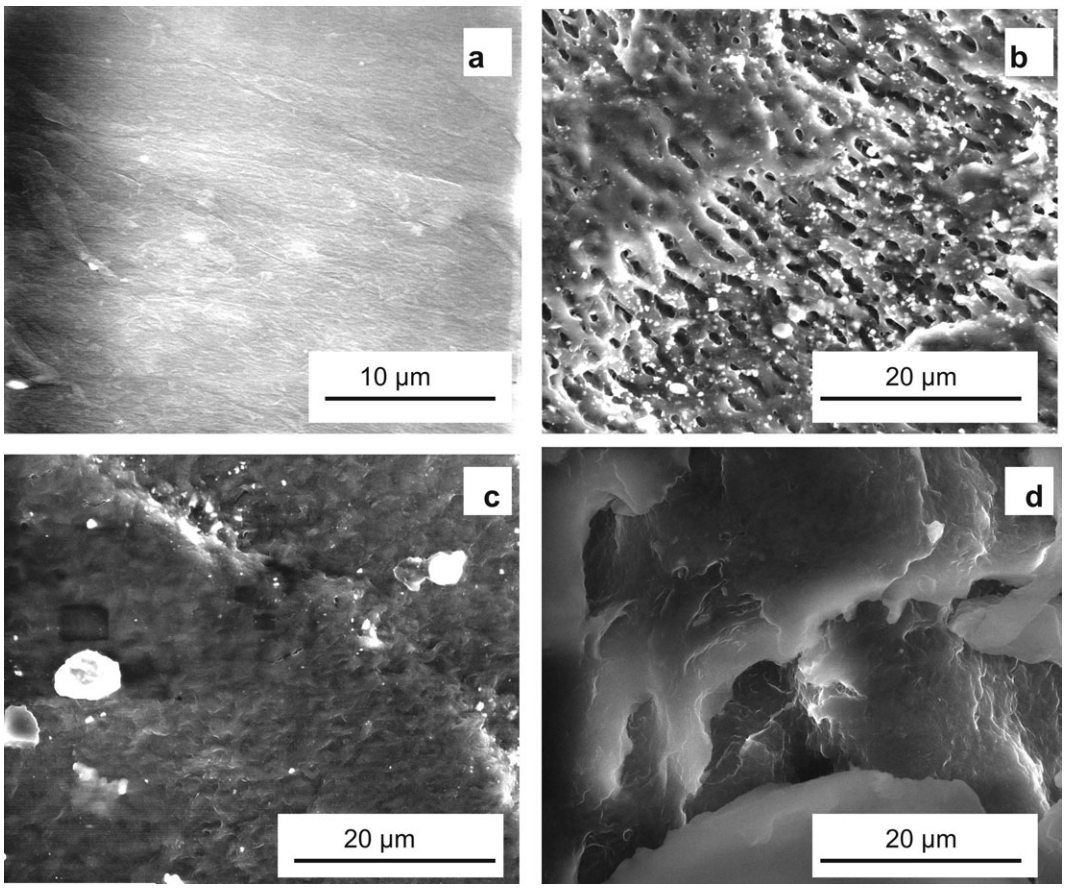

Figure 8. SEM images of rTPU surface with 3 wt % of C30B before (a) and after hydrolytic degradation at 150 h (b), 400 h (c), and 800 h (d) (magnification ×5000).

Table IV. Influence of Hydrolytic Degradation on the Molecular Weights and Molecular Weights Distribution of rTPU and rTPU/C30B Nanocomposite with 5 wt % of Clay

Sample	Time of hydrolytic degradation (h)	M_n (g mol^{-1})	M_w (g mol^{-1})	M_w/M_n
rTPU	0	4752	11,116	2.339
rTPU	670	2173	30,654	14.101
rTPU/C30B	0	53,167	221,673	4.169
rTPU/C30B	670	2389	77,725	32.531

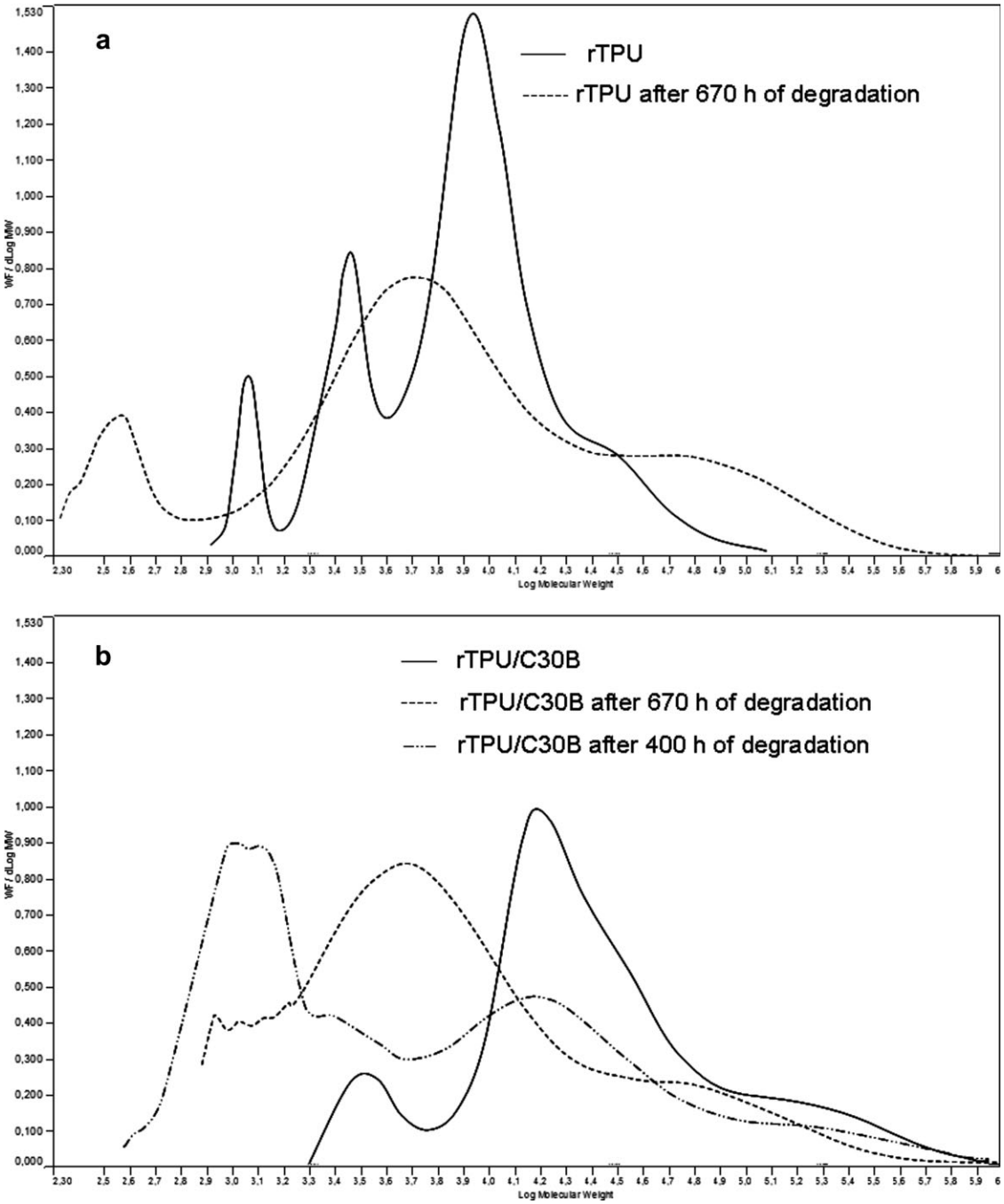

Figure 9. SEC curves of rTPU (a) and rTPU/C30B = 95/5 wt % nanocomposite (b) before and after hydrolytic degradation.

Applied Polymer SCIENCE

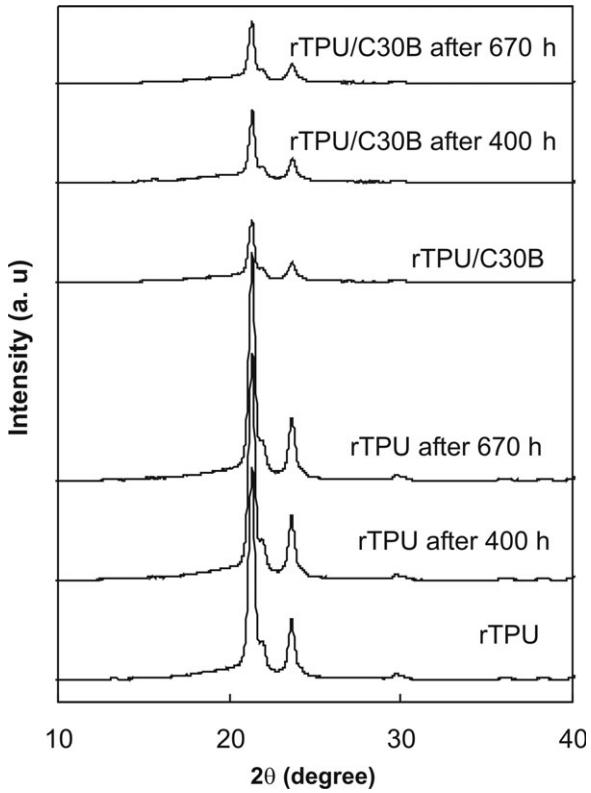

Figure 10. X-ray diffractograms of rTPU and rTPU/C30B nanocomposites with 5 wt % of clay before and after hydrolytic degradation.

biodegradation reaction that leaving behind material rich in the crystalline phase.

CONCLUSIONS

In this work the effect of the mastication time and the organically modified MMT (i.e., C10A, C15A, and C30B) content on the morphology, melt flow, mechanical properties, and hydrolytic degradation of polycaprolactone-based thermoplastic polyurethane (rTPU) were investigated. The melt flow, tensile and flexural properties of rTPU decrease with increasing mastication time, while thermal properties are only affected slightly by the recycling process.

The nature of the organomodifier of MMT strongly influenced the properties of the rTPU/MMT composites. The lack of strong polar interaction between the ammonium cations in C15A and rTPU chains prevents polymer intercalation; meantime C30B has strong polar interaction with rTPU matrix, facilitating the intercalation of rTPU chains into clay pallets and formation of the delaminated rTPU/C30B nanocomposites. Incorporation of MMT fillers in rTPU matrix decreases melt flow properties, tensile strength, and elongation at break, however, increases modulus and hydrolytic degradation rate. The investigation of molecular weight changes shows that MMT increase the weight loss and polydispersity of rTPU during degradation.

Hydrolysis leads to the increase of the crystallinity of rTPU matrix and rTPU/C30B nanocomposites, though MMT even retards rate of crystallinity change during time of hydrolytic degradation.

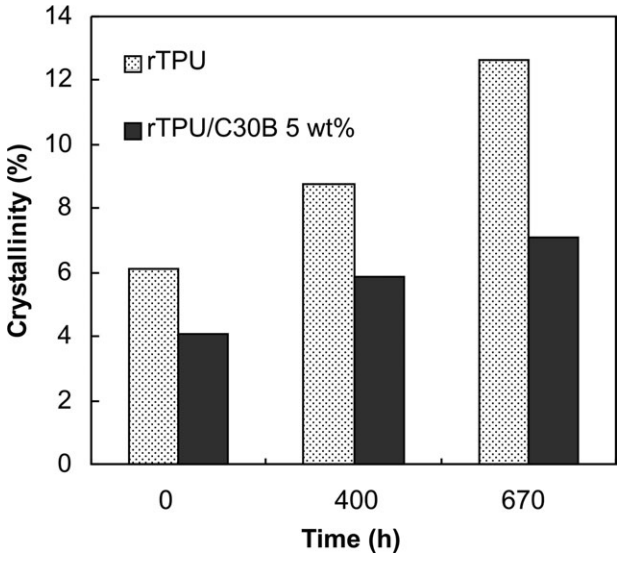

Figure 11. Changes of the crystallinity upon hydrolysis time for rTPU and rTPU/C30B nanocomposite with 5 wt % of clays.

REFERENCES

1. Jeong, E. H.; Yang, J.; Lee, H. S.; Seo, S. W.; Baik, D. H.; Kim, J.; Youk, J. H. *J. Appl. Polym. Sci.* **2008,** *107*, 803.
2. Rodrigues da Silva, G.; Armando da Silva-Cunha, J.; Behar-Cohen, F.; Ayres, E.; Orefice, R. L. *Polym. Degrad. Stab.* **2010,** *95*, 491.
3. Rutkowska, M.; Jastrebska, M.; Janik, H. *React. Funct. Polym.* **1998,** *38*, 27.
4. Woodruff, M. A.; Hutmacher, D. W. *Prog. Polym. Sci.* **2010,** *35*, 1217.
5. Fukushima, K.; Abbate, C.; Tabuani, D.; Gennari, M.; Rizzarelli, P.; Camino, G. *Mater. Sci. Eng. C Mater.* **2010,** *30*, 566.
6. Abdel-Rehim, H. A.; Yoshii, F.; Kume, T. *Polym. Degrad. Stab.* **2004,** *85*, 689.
7. Sun, H.; Mei, L.; Song, C.; Cui, X.; Wang, P. *Biomaterials* **2006,** *27*, 1735.
8. Bosworth, L. A.; Downes, S. *Polym. Degrad. Stab.* **2010,** *95*, 2269.
9. Hoshino, J.; Limpanart, S.; Khunthon, S.; Osotchan, T.; Traiphol, R.; Srikhirin, T. *Mater. Chem. Phys.* **2010,** *123*, 706.
10. Bordes, P.; Pollet, E.; Averous, L. *Prog. Polym. Sci.* **2009,** *34*, 125.
11. Jimenez, G.; Ogata, N.; Kawai, H.; Ogihara, T. *J. Appl. Polym. Sci.* **1997,** *64*, 2211.
12. Mondragón, M.; Sánchez-Valdés, S.; Sanchez-Espíndola, M. E.; Rivera-López, J. E. *Polym. Eng. Sci.* **2011,** *51*, 641.
13. Lee, S. R.; Park, H. M.; Lim, H.; Kang, T.; Li, X.; Cho, W. J.; Ha, C. S. *Polymer* **2002,** *43*, 2495.

14. Ku, B. C.; Froio, D.; Steeves, D.; Kim, D. W.; Ahn, H.; Ratto, J. A.; Blumstein, A.; Kumar, J.; Samuelson, L. A. *J. Macromol. Sci. Pure Appl. Chem.* **2004,** *41*, 1401.
15. Sung, J. H.; Mewis, J.; Moldenaers, P. *Korea–Aust. Rheol. J.* **2008,** *20*, 27.
16. Alexandre, M.; Dubois, P. *Mater. Sci. Eng.* **2000,** *28*, 1.
17. Narenda, K. S.; Biswapratim, D. P.; Jagat, K. R.; Rathindra, M. B.; Madhu, Y.; Gajendra, S.; Sudip, M.; Pralay, M. *ACS Appl. Mater. Inter.* **2010,** *2*, 69.
18. Zou, H.; Ran, Q.; Wu, S. *J. Polym. Compos.* **2008,** *29*, 385.
19. Pavlidou, S.; Papaspyrides, C. D. *Prog. Polym. Sci.* **2008,** *33*, 1119.
20. Leone, G.; Bertini, F.; Canetti, M.; Boggioni, L.; Stagnaro, P.; Tritto, I. *J. Polym. Sci. A Polym. Chem.* **2008,** *46*, 5390.
21. Liang, G.; Xu, J.; Bao, S.; Xu, W. *J. Appl. Polym. Sci.* **2004,** *91*, 3974.
22. Zhao, Z.; Tang, T.; Qin, Y.; Huang, B. *Langmuir* **2003,** *19*, 7157.
23. Thomas, P. C.; Tomlal, J. E.; Selvin, T. P.; Thomas, S.; Joseph, K. *Polym. Compos.* **2010,** *31*, 1515.
24. Altpeter, H.; Bevis, M. J.; Grijpma, D. W.; Feijen, J. *J. Mater. Sci. Mater. Med.* **2004,** *15*, 175.
25. Jankauskaitė, V.; Laukaitienė, A.; Mickus, V. K. *Mater. Sci. Medzg.* **2009,** *5*, 142.
26. Cheary, R. W.; Coelho, A. A. Available at: http://www.ccp14.ac.uk/tutorial/xfit-95/xfit.htm.
27. Jankauskaitė, V.; Žukienė, K.; Betingytė, V.; Laukaitienė, A. *Struct. Polym. Compos. Monogr. (in Polish)* **2011**, 193.
28. Mishra, A. K.; Chattopadhyay, S.; Rajamohanan, P. R.; Nando, G. B. *Polymer* **2011,** *52*, 1071.
29. Zhoua, Q.; Xanthos, M. *Polym. Degrad. Stab.* **2008,** *93*, 1450.
30. Maiti, P.; Batt, C. A.; E. P. Giannelis, E. P. *Biomacromolecules* **2007,** *8*, 3393.
31. Lee, J. H.; Park, T. G.; Park, H. S.; Lee, D. S.; Lee, Y. K.; Yoon, S. C.; Nam, J. *Biomaterials* **2003,** *24*, 2773.
32. Rutkowska, M.; Krasowska, K.; Heimowska, A.; Steinka, L.; Janik, H.; Haponiuk, J.; Karlsson, S. *Pol. J. Environ. Stud.* **2002,** *11*, 413.